AIAA JOURNAL
Vol. 33, No. 5, May 1995

Failure of Tapered Composites Under Static and Fatigue Tension Loading

Michael R. Wisnom,* M. I. Jones,† and Weicheng Cui‡
University of Bristol, Bristol BS8 1TR, England, United Kingdom

One glass fiber-epoxy and two carbon fiber-epoxy rapidly tapered sections with dropped 0- and ±45-deg plies have been designed, manufactured, and tested. Under static loading, close to net section tensile strength was achieved. The glass fiber taper also achieved net section strength under tension fatigue loading, but the carbon fiber tapers showed a significant reduction in fatigue strength due to delamination from the ends of the terminating 0-deg plies. The most significant factor controlling strength is the number of plies dropped together. Unidirectional dropped plies are much more susceptible to delamination than ±45-deg plies. Satisfactory strength predictions can be made for both static and fatigue tension loading based on net section stresses and a simple equation for the strain energy release rate. This approach looks promising as the basis for a general method for designing tapered composites.

I. Introduction

TAPERED sections involving the progressive dropping of plies are prone to delamination, especially under fatigue loading. Such tapered sections are very commonly used to achieve changes in thickness. A typical example is a helicopter rotor blade, where increased thickness is necessary near the root. Normally a short tapered transition region is desirable. However, due to the lack of reliable methods for predicting delamination, a very gradual taper is usually used.

A number of authors have investigated static strength of tapered laminates.[1–8] However, there is no consensus on how to predict failure. Various approaches have been proposed based on maximum stresses,[2] stresses averaged over a distance,[6] stresses evaluated at a characteristic distance,[8] and strain energy release rates.[5] Several investigations on tension fatigue of tapered specimens have been published.[9–11] The problem of predicting fatigue strength has not received very much attention, although in the latter study a method was proposed for predicting onset of unstable delamination based on strain energy release rate analysis.[11]

A program of research has been undertaken at Bristol University to investigate failure in tapered composites under static and fatigue loading. A series of tests on very simple symmetric specimens have enabled failure mechanisms to be studied.[12] Much of the work has been on unidirectional material, avoiding some of the potential problems with edge effects. It has been found that the dominant failure mechanism for these specimens is delamination initiating above and below the ends of the terminating plies and propagating into the thick section along the interface between continuous and discontinuous plies. The results have indicated that the most important parameter affecting failure is the strain energy release rate associated with the terminating plies.

Based on this work, a method has been proposed for predicting static strength of tapered specimens. A simple equation is used for calculating the strain energy release rate. This is then compared with a value of fracture energy deduced from a tension test on a constant thickness unidirectional specimen with the central plies cut across the complete width. Satisfactory correlation has been obtained for tapered unidirectional glass fiber-epoxy specimens under static tension and compression loading.[13]

Received July 31, 1993; revision received April 25, 1994; accepted for publication May 18, 1994.

*Reader, Department of Aerospace Engineering.
†Experimental Officer, Department of Aerospace Engineering.
‡Research Associate, Department of Aerospace Engineering; currently, Research Engineer, China Ship Scientific Research Centre, Wuxi, Jiangsu 214082, People's Republic of China.

Tension fatigue tests on similar specimens have shown that the failure mechanisms are similar to those under static loading.[14] However, delamination propagates immediately, and so it is necessary to consider delamination rates. This suggests that a similar approach could be used for predicting fatigue strength as for static strength, based on the simple equation for the strain energy release rate and experimental data for delamination rates. Fatigue data could be obtained from tension tests on the same constant thickness unidirectional specimens with cut central plies as used in the static tests to measure fracture energy.

To assess the validity of this approach for more realistic tapered geometries involving ±45-deg as well as 0-deg dropped plies, three types of rapidly tapered specimens have been produced and tested. The tapers have been designed to achieve maximum strength under both static and fatigue tension loading. This paper presents the results of the tests carried out on these specimens to determine strength and investigate failure mechanisms. Comparisons are made between predicted and measured strengths, and it is found that correlation is good for both static and fatigue loading.

II. Design of Tapered Specimens

Three symmetric specimens were designed, each with a thick section at both ends and two tapers down to a central thin section. The sections were designed with thickness ratios typical of those at the root of a helicopter rotor blade. One carbon fiber-epoxy and one glass fiber-epoxy specimen were designed for maximum strength with a rapid taper angle. Calculations indicated that these were both likely to fail as a result of fiber breakage under static loading, and so a second carbon epoxy specimen was designed deliberately to delaminate to validate the delamination predictions. The same number of plies were used but dropped in a different way. The taper angle was also changed to be more shallow. This was done to demonstrate that the angle is not the critical factor determining failure.

Figure 1 shows schematically one end of the tapered glass fiber section. There are eight 0-deg plies in the thin section. The thick section contains eight 0-deg and six pairs of ±45-deg plies. This gives a transition from a nominal thickness of 2.5 mm down to 1 mm. To maximize strength, the ±45-deg plies were dropped in six single pairs, with continuous interleaving 0-deg plies between them. Plies were dropped symmetrically in three steps, with the plies closest to the midplane terminating at the thin end. To investigate the effect of the taper angle, different values of the distance d between dropped plies were used at each end of the specimen. At one end a spacing of 1 mm was used, producing a tapered section only just over 2 mm long, with a theoretical angle between the outside surface and the centerline of about 16 deg. A spacing of 2 mm was used at the other end, producing a tapered section of just over

4 mm at this end and an angle of about 8 deg. The layup in the thick section is $[(0/\pm\bar{4}5)_3/0]_s$, where the bar indicates the dropped plies.

The first carbon specimen is shown schematically in Fig. 2. It has 16 0-deg plies in the thin end. The thick end has 24 0-deg plies and 12 pairs of ±45-deg plies. This gives a nominal thickness transition from 6 to 2 mm. Plies were dropped symmetrically about the centerline, with the 0-deg plies dropped closest to the thin end, and then the ±45-deg plies. The 0-deg plies were dropped singly, and the ±45-deg plies were dropped in single pairs except for one double pair at the center. Calculations suggested that failure was likely to occur by fiber breakage at the first dropped ply from the thin end. To maximize fiber strength, plies closest to the thin end were dropped from the outside, with a single overlaid continuous ply. This meant that the middle 14 plies were straight, whereas if plies near the thin end had been dropped further inside the specimen, more plies would have been kinked. The layup in the thick section is $[0/\pm\bar{4}5/\bar{0}/\pm\bar{4}5/(0/\bar{0})_3/(0/\pm\bar{4}5)_4]_s$. A spacing of 1 mm was used between the plies dropped singly and 2 mm between those dropped in pairs, producing a tapered section about 14 mm long with an angle of about 8 deg on either side of the center.

The second carbon section is shown in Fig. 3. It has a more conventional arrangement with plies dropped from the inside at the thin end. To ensure delamination, both 0-deg and ±45-deg plies were dropped in pairs. The ±45-deg plies were dropped closest to the thin section, and the drop at the start of the taper is actually a double pair at the midplane. The resulting layup in the thick section is $[(0/\bar{0}_2)_2/(0/\pm\bar{4}5)_6]_s$. A spacing between pairs of dropped plies of 4 mm was used, giving a tapered section about 28 mm long with an angle of about 4 deg.

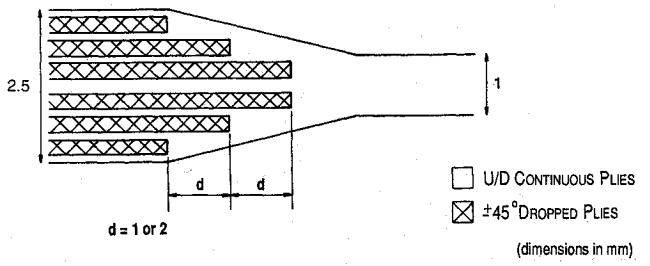

Fig. 1 Schematic representation of glass/epoxy rapid tapered specimen.

III. Prediction of Strength

Static

Prediction of delamination is based on calculation of the strain energy release rate from a simple equation and comparing it with a value for the fracture energy. This method has been found to give good predictions of delamination strength for simple unidirectional tapered sections.[13]

Assuming a particular delamination location, the strain energy release rate G can be calculated in terms of the applied load per unit width P by

$$G = P^2(K_0 - K^*)/4K_0K^* \tag{1}$$

where K_0 is the in-plane stiffness of the section before delamination, defined as the axial force per unit width for unit applied axial strain, and K^* is the stiffness after delamination assuming that the delaminated plies carry no load and that the remaining blocks of material

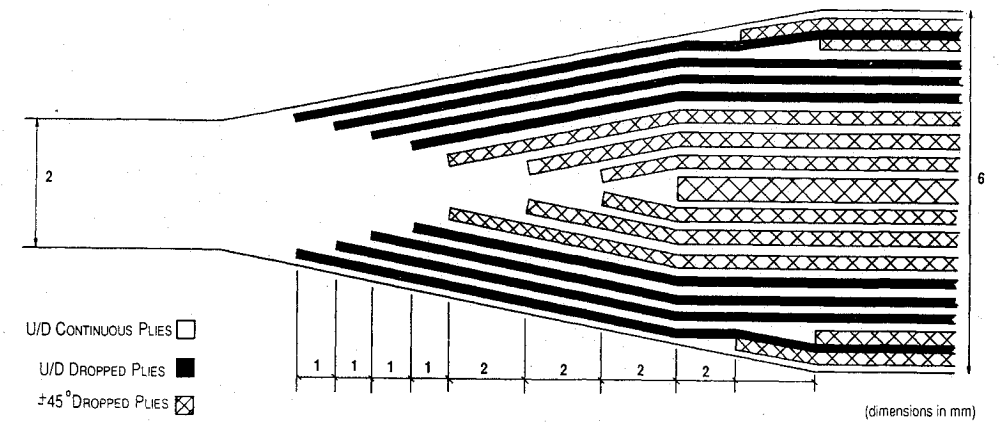

Fig. 2 Schematic representation of carbon/epoxy rapid tapered specimen type 1.

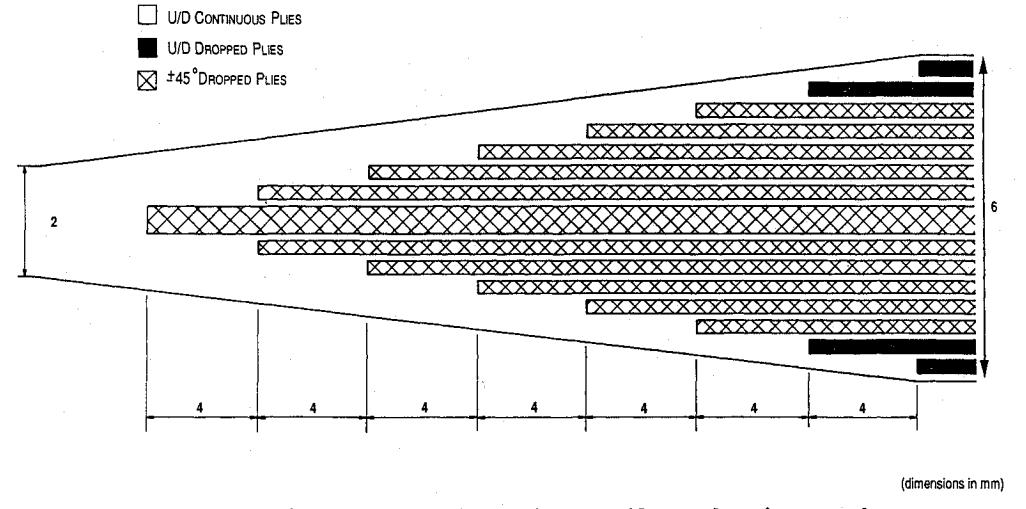

Fig. 3 Schematic representation of carbon/epoxy rapid tapered specimen type 2.

Table 1 Assumed material properties

Property	Glass-epoxy	Carbon-epoxy
0 deg Young's modulus (GPa)	43.9	138.0
90 deg Young's modulus (GPa)	15.4	9.65
Poisson's ratio	0.3	0.26
Shear modulus (GPa)	4.34	5.0

are unconnected. The derivation of this equation is given in the Appendix. Where there are only 0-deg plies, K is simply the product of the fiber direction modulus and the thickness. Where ±45-deg plies contribute to the stiffness, K can be calculated by laminated plate theory. Nominal thicknesses are used rather than actual values to try to correct for differences due to variations in the amount of resin present that are not expected to affect stiffness significantly. A ply thickness of 0.127 mm is used, corresponding to 60% volume fraction. Material property data are given in Table 1.

If all blocks of dropped plies are the same, then the highest strain energy release rate will be for delamination at the block nearest the thin section. For the glass fiber specimens delamination will therefore occur at the forward dropped plies closest to the thin section. Since the specimen is symmetric, it is assumed that the two blocks of plies on either side of the centerline delaminate simultaneously. Using Eq. (1) enables G to be calculated in terms of the stress in the thin section σ. This then needs to be divided by two to get the strain energy release rate associated with each delamination:

$$G = 4.26 \times 10^{-7}\sigma^2 \tag{2}$$

A value of fracture energy of 1.08 N/mm is used, based on the measured delamination propagation stress for a 10-ply unidirectional specimen with the middle two plies cut across the width.[12] Tests on different types of specimens did show some differences in effective fracture energy. It was noticed that thicker specimens tended to give higher values than thinner ones. Use of a value from a 10-ply specimen for predicting strength of thicker specimens should be conservative. Equating this with the strain energy release rate from Eq. (2) gives a predicted delamination stress of 1592 MPa. Available data for fiber direction tensile strength of plain specimens corrected to 60% volume fraction indicated a strength of 1381 MPa. These specimens were therefore expected to fail due to fiber breakage before any delamination.

For the first type of carbon specimen, three possible delamination sites need to be considered: the dropped 0-deg plies nearest the thin end, the dropped pairs of ±45-deg plies nearest the thin end, and the middle block of two pairs of ±45-deg plies. The first case was found to be critical. Using Eq. (1) gives

$$G = 2.045 \times 10^{-7}\sigma^2 \tag{3}$$

A value of fracture energy of 0.82 N/mm is used, obtained from the same type of specimen as for glass epoxy.[14] This gives a predicted delamination stress of 2002 MPa. Available data for fiber direction tensile strength corrected to 60% volume fraction indicated a fairly similar value of 2105 MPa, suggesting that this specimen may fail either by delamination or fiber fracture.

For the second type of specimen, delamination at the drop of 0-deg plies nearest the thin end is most critical. Laminated plate theory is used to calculate the stiffness of the whole section at this location before delamination. The layup here is effectively $[0_2/\bar{0}_2/(0/\pm\bar{45})_6]_s$ because the other two pairs of 0-deg plies have already been dropped. After delamination the stiffness of the center section of layup $[(0/\pm\bar{45})_6]_s$ is calculated in the same way. The outside two pairs of continuous unidirectional plies are assumed to still carry load but to act independently from the rest of the section with the same fiber direction strain. Their stiffness is therefore calculated separately and added to produce the total stiffness after delamination. Dividing the total strain energy release rate by two, the value associated with one delamination is

$$G = 2.686 \times 10^{-7}\sigma^2 \tag{4}$$

Table 2 Predicted delamination rates

Specimen type	Max stress (MPa)	da/dN (mm/cycle)
Glass	862	1.18×10^{-4}
Glass	984	9.06×10^{-4}
Carbon type 1	638	1.0×10^{-7}
Carbon type 1	757	1.0×10^{-6}
Carbon type 1	1063	1.0×10^{-4}
Carbon type 2	660	1.0×10^{-6}
Carbon type 2	928	1.0×10^{-4}

Using the fracture energy of 0.82 N/mm gives a predicted thin section delamination stress of 1747 MPa. Since the predicted delamination stress is significantly lower than the fiber direction tensile strength, this specimen is expected to fail by delamination.

Fatigue

Predictions of delamination rates are based on fatigue tests carried out on the same constant section specimens with cut internal plies as were used for determining the fracture energy.

Specimens with eight continuous and two cut plies were tested in tension-tension fatigue at an R ratio of minimum to maximum stress of 0.1. The delamination length was estimated based on the change in stiffness measured with an extensometer and plotted against cyclic strain energy release rate amplitude. The latter was calculated from the applied load and theoretical stiffness using Eq. (1). The data were found to lie close to a straight line on a log-log plot. The following equations were obtained by least-squares fitting of the data:

$$\frac{da}{dN} = 0.647\,\Delta G^{7.42} \tag{5}$$

for glass fiber epoxy and

$$\frac{da}{dN} = 2.14\,\Delta G^{6.77} \tag{6}$$

for carbon fiber epoxy. Full details of the tests can be found elsewhere.[14]

Using Eqs. (2) and (5) for the glass specimens, and Eqs. (3), (4), and (6) for the carbon specimens, delamination rates can be predicted. These results are shown in Table 2. For the carbon specimens stresses were chosen to give delamination rates of between 10^{-4} and 10^{-7} mm/cycle. For the glass specimens the stresses were chosen after the static tests had been carried out, and the values of 862 and 984 MPa correspond to about 70 and 80% of the static strength.

Comparison with plain section fatigue data showed that for the carbon fiber specimens no problems would be expected due to fiber fatigue. However, for the glass fiber specimens, the data indicated that fiber failure could be expected after about 6900 cycles at 862 MPa and after about 2100 cycles at 984 MPa.

IV. Experimental

Specimen Manufacture

The materials used were Ciba-Geigy E glass/913 and XAS/913 prepregs, typical materials used in helicopter rotor blades. Both materials are based on the same 125°C cure modified epoxy resin matrix.

Panels were made using a ply in-fill technique whereby an equivalent tapered section is built up on the other side of the release cloth. This is illustrated for a simple taper in Fig. 4. The technique allows panels to be made between flat plates, producing good consolidation without the need for special tooling.

Figure 5 shows the edge of the shallower end of the glass fiber tapered specimen. The triangular resin pockets in front of the dropped plies are clearly visible. No voids could be seen.

The actual thicknesses of the glass fiber specimens were slightly higher than the nominal values. The thick sections were between 2.78 and 2.89 mm and the thin sections between 1.16 and 1.19 mm. This compares with thicknesses of 2.54 and 1.016 mm based on a ply thickness of 0.127 mm. The carbon specimens varied between 5.90 and 6.28 mm in the thick section and from 2.06 to 2.12 mm

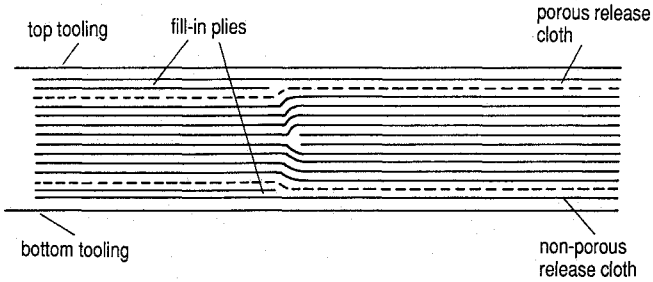

Fig. 4 Manufacturing method for tapered specimens.

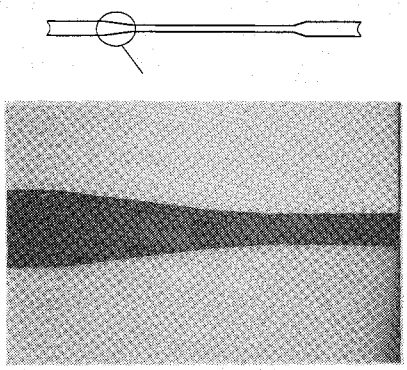

Fig. 5 Edge of shallow end of tapered glass fiber specimen.

in the thin section. These are closer to the thicknesses of 6.096 and 2.032 mm based on the nominal ply thickness of 0.127 mm.

For the steeper end of the glass fiber specimens, the measured angle between the outside surface and the centreline was about 12 deg, slightly less than the theoretical angle of 16 deg. However, for the shallower end, the measured angle of 7.5 deg was very close to the nominal value of 8 deg. For the two carbon fiber tapers, the measured angles were also close to the nominal values of 8 and 4 deg, respectively.

Specimens 10 mm wide were cut out of the panels with a diamond wheel. Earlier work on constant thickness glass fiber epoxy with cut ±45-deg plies under tension fatigue loading had not shown any significant difference in delamination behavior between specimens of width 10 and 20 mm.[14] Although free edge effects might be expected to be significant, calculations based on laminated plate theory show that the strain energy release rate associated with the discontinuous plies is much greater than that due to the edge effect, and so it is the former that drives the delamination. The use of relatively narrow specimens was therefore judged to be acceptable.

For the glass fiber and first carbon fiber specimens, a specimen length of 200 mm was used and 250 mm for the second carbon type. All specimens had a thin section of about 30 mm between the two tapers. Emery paper was wrapped around the end 50 mm of the specimens to protect them in the grips. However, on the first glass fiber static test a few fiber breaks occurred at the grips, and so the rest of the glass specimens for the static tests were tabbed with 50-mm-long glass fiber cross-plied tabs.

The edges of the specimens were lightly polished by rubbing them on emery paper on a flat surface to facilitate inspection for damage.

Static Tests

All specimens were tested in an Instron servo-hydraulic test machine under displacement control at a cross-head speed of 0.5 mm/min.

Five glass fiber specimens were tested. The first three were loaded to failure. The fourth was stopped just as failure was starting, and the fifth was stopped before any damage was visible.

Four specimens of each of the carbon tapers were tested to failure. A fifth specimen of the first type was loaded nearly to failure and then unloaded for inspection.

The edges of the specimens that did not fail completely were examined under an optical microscope. For the carbon fiber specimen it was necessary to use a fluorescent dye penetrant in order to detect any damage.

Fatigue Tests

All fatigue tests were carried out in an Instron servo-hydraulic test machine under load control with an R ratio of 0.1. For tests at different severities, the frequency was varied inversely with the maximum stress to keep the stress rate in the thin section the same. The frequency was kept sufficiently low to avoid any significant heating in the specimens. For the carbon specimens the rate was between 7 and 11.8 Hz, and for the glass it was 1.75 or 2 Hz. A lower rate was used for the latter specimens because of the higher strains due to the lower modulus.

Three glass fiber-epoxy specimens were tested at a maximum stress of 862 MPa. One specimen was also tested at 984 MPa maximum stress. Tests were carried out to failure.

For the carbon fiber tapers, tests were taken to a fixed number of cycles and stopped before catastrophic failure occurred. For the first type of specimen two tests were carried out at a maximum stress of 1063 MPa for 10^4 cycles, and one each at 757 MPa for 10^6 cycles and 638 MPa for 10^7 cycles. For the second type of specimen two tests were carried out at a maximum stress of 928 MPa for 10^4 cycles. It was intended to test another specimen at 660 MPa for 10^6 cycles, but in fact this test continued up to 2.3×10^6 cycles. The applied stresses were calculated based on producing 1 mm of delamination in 10^4, 10^6, and 10^7 cycles.

To try to assess the development of damage, one carbon specimen of the first type was cycled at 1080 MPa, and the test stopped periodically to inspect for damage. Two specimens of the second type were also tested in this way with a maximum stress of 917 MPa. It was rather difficult to see cracks and virtually impossible to obtain accurate crack length measurements. On one of the specimens typing correction fluid was applied in an attempt to make the cracks more visible. After testing, the carbon specimens were examined using fluorescent dye penetrant. However, this was not used during the fatigue tests because of fears that it might influence the delamination behavior.

V. Results

Static Tests

Results are summarized in Table 3. Failure stresses are calculated from the actual width and nominal thickness of the thin section based on a ply thickness of 0.127 mm. The results were very repeatable, as can be seen from the low coefficients of variation in the range 1–4%.

For the glass fiber specimens, in most cases no damage was seen until complete failure occurred. Specimens exhibited a brushlike failure mode, with considerable damage distributed over a large area. Most of the fiber breaks appeared to occur near the thin ends of the tapers, with a greater proportion at the steeper taper. A few fiber breaks also occurred near the grips, although failure did not initiate there. There was some evidence of delamination of the specimens between plies, but this is believed to have happened after failure initiated.

The first three specimens were tested to ultimate failure. With specimen 4 it was possible to stop the test when fiber breaks initiated but before complete failure. In contrast to what would have been expected based on the earlier tests, the fiber breaks occurred at the shallower end, with no breaks visible at the steeper taper.

Specimen 5 was loaded to 1176 MPa and unloaded before any damage was apparent. Inspection under the optical microscope

Table 3 Static failure stresses (MPa)

Specimen no.	Glass	Carbon type 1	Carbon type 2
1	1227	2246	1756
2	1260	2042	1874
3	1234	2191	1828
4	(1201)	2202	1880
Average	1240	2170	1834
c.v.	1.4%	4.1%	3.1%

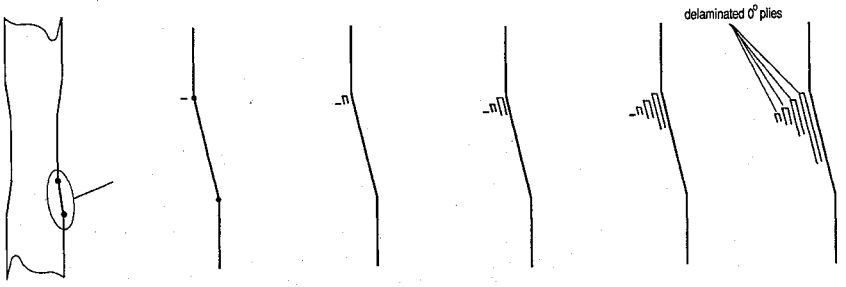

Fig. 6 Schematic representation of delamination growth in carbon/epoxy taper type 1.

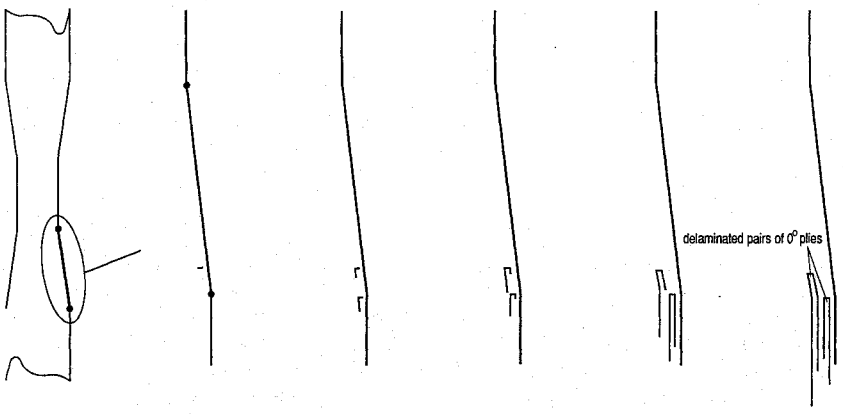

Fig. 7 Schematic representation of delamination growth in carbon/epoxy taper type 2.

showed that there were cracks in the forwardmost resin pockets at both ends of the specimen. The cracks were perpendicular to the loading direction, about 0.25 mm in front of the ends of the discontinuous plies. There was also a crack in one of the middle group of resin pockets. No cracks could be seen in the resin pockets in front of the rearmost dropped plies. No delamination was visible.

Carbon fiber specimens of type 1 failed catastrophically with no indication of any damage before complete failure. The specimens showed less splitting than the glass ones. Most of the fiber breaks were concentrated around the thin end of one of the tapers, with no fiber failures at the grips.

A fifth specimen was loaded to 2000 MPa and unloaded before any damage was seen. Examination with dye penetrant showed that there were cracks in the resin pockets at the forwardmost dropped plies, but no cracks at any of the other dropped plies. No delamination could be seen.

For the carbon fiber specimens of the second type, first failure was not catastrophic. There was a sharp drop in load, and the two surface plies on one side delaminated along most of the gauge length and fractured. The specimens still carried about 1500 MPa after initial damage. Two tests were taken further. On one specimen a similar failure occurred on the other side, whereas the other specimen failed catastrophically. From all of the observations it appeared that failure had initiated by delamination into the thick section at the forwardmost pair of 0-deg plies. Delamination then propagated into the thin section, and the surface plies also failed. Cracks in the resin pockets were visible at the forwardmost plies on the other side of the specimen. In some cases delamination could also be seen above and below these plies starting from the resin crack, propagating into the thick section, although the amount of delamination varied greatly. No damage was seen at any of the ±45-deg dropped plies except for a matrix crack at the first block of two pairs of ±45-deg plies.

Fatigue Tests

Table 4 summarizes the results for the glass fiber specimens. All of these specimens failed catastrophically due to fiber fatigue. No significant fiber damage was seen before final failure. Most of the breaks were concentrated around the thin end of the steeper taper. On specimen 3 a small amount of delamination was visible at the shallower taper after around 8800 cycles, about two thirds of the way through the test. As on the static tests, failure was accompanied by a large amount of damage, and so little further information could be gained from inspection of the failed specimens.

Table 4 Fatigue results for glass fiber specimens

Specimen number	Max stress (Mpa)	Cycles to failure
1	862	13,377
2	862	15,796
3	862	12,447
4	984	3,033

Table 5 summarizes the results for the carbon fiber specimens. The number of delaminations visible at the edges of each specimen was counted at the end of the test after applying dye penetrant. For the specimens of type 1 there are 8 dropped 0-deg plies at each end, giving a total of 16 delamination sites. Since these could be observed on both edges of the specimen, the maximum number of 0-deg ply delaminations was 32. For the specimens of type 2, since there were only four pairs of dropped 0-deg plies at each end, the maximum number of 0-deg delaminations was 16. Longest delamination crack lengths are also given.

The initial carbon specimen of type 1 was stopped periodically and examined with a traveling microscope. From this and closer inspection with dye penetrant at the end of the test, a picture of the way in which damage progresses could be built up. The first damage to occur is a crack across the resin pocket at one of the forwardmost 0-deg plies. This progresses to delamination, and then a crack initiates in the resin pocket at the next dropped 0-deg ply. This continues, with the forwardmost 0-deg ply always having the longest delamination. Figure 6 shows the damage schematically. No delamination or cracking in the resin pockets was seen for any of the ±45-deg dropped plies. No delamination forward into the thin section was observed. Similar damage was observed in the other tests, which were all stopped before complete failure.

The carbon specimens of type 2 behaved similarly, with again damage initiating at the forwardmost 0-deg dropped ply. Figure 7 shows schematically the development of damage observed from the first two specimens. The delamination was more similar between the forwardmost and second block of dropped plies, and in some cases the cracks were longer at the second block. There was also a noticeable tendency for the delaminations associated with a particular block of dropped plies to be longer on the interior side than

Table 5 Fatigue results for carbon fiber specimens

Specimen type	Specimen number	Max stress (MPa)	No. of cycles	No. of delam. cracks	Longest cracks (mm)
1	1	1080	104,861	25	8.4
1	2	1063	10,000	12	2.4
1	3	1063	10,000	13	1.7
1	4	757	1,000,000	6	1.3
1	5	638	10,000,000	4	0.5
2	1	917	282,247	16	44
2	2	917	254,762	12	41
2	3	928	10,000	6	1.7
2	4	928	10,000	12	0.7
2	5	660	2,319,501	5	1.1

on the exterior side. As with the first type of specimen, there was no observable damage at any of the dropped ±45-deg plies and no delamination into the thin section.

VI. Discussion

Static Tests

The glass fiber specimens and carbon fiber specimens of type 1 all failed by fiber fracture. For the glass fiber specimens, the stress of 1240 MPa achieved in this rapidly tapered section is only about 10% less than the plain section tensile strength of 1381 MPa. For the carbon fiber specimens, the failure stress of 2170 MPa actually exceeds the nominal plain section strength of 2105 MPa by 3%. Measurement of ultimate tensile strength is difficult because of the problem of introducing stress concentrations where the specimen is gripped. The true tensile strength of XAS/913 is believed to be significantly higher than 2105 MPa.

Finite element analysis indicates that there is a severe stress concentration immediately in the vicinity of the dropped plies, but this appears to have relatively little effect on tensile strength. This is thought to be because the high stresses only extend over a very small volume of material, and the stress gradients are high. Close to net section tensile strength can be achieved in these materials provided plies are dropped singly, or in pairs for ±45-deg plies, and continuous plies are interleaved between the dropped plies. This is consistent with the results in Ref. 3 where it was reported that dropped plies did not have a significant effect on tensile strength of graphite/epoxy.

The second type of carbon specimen was deliberately designed to delaminate by dropping 0-deg plies in pairs. These specimens did delaminate, as expected. The failure mechanism was very similar to that seen on simpler specimens, with delamination occurring above and below the terminated plies, into the thick section.

Delamination occurred towards the thick end of the taper, at the forwardmost 0-deg drop rather than at the thin section at the forwardmost ±45-deg drop. This happened despite the higher stress close to the thin section and the drop of four 45-deg plies together compared with just two 0-deg plies dropped together. These results confirm the much greater susceptibility to delamination of 0-deg dropped plies compared with ±45-deg dropped plies.

The first type of carbon fiber specimen was significantly stronger than the second type despite the fact that the taper angle was much steeper. This suggests that the angle is not particularly important where there are continuous plies interleaved between the discontinuous ones. However, if the angle was too steep, there would be a risk of delamination occurring into the thin section.

Fatigue Tests

The glass fiber specimens failed by fiber fatigue, consistent with the fiber failure mode obtained under static loading. The number of cycles to failure was actually somewhat higher than expected on the basis of plain section fatigue data. Earlier work on simpler specimens with terminated plies showed fatigue strength similar to that of plain unidirectional specimens.[14] As found for static loading, the stress concentration at the end of the terminated plies does not appear to have a significant effect on strength.

On the basis of the predicted delamination rates given in Table 2, delamination of around 1–3 mm would have been expected

Table 6 Correlation of results for static strength

Specimen type	Taper angle	Predicted failure stresses (MPa)		Measured strength (MPa)	Failure mode
		fiber	Delamination		
Glass	12 deg	1381	1592	1240	fiber failure
Carbon 1	8 deg	2105	2002	2170	fiber failure
Carbon 2	4 deg	2105	1747	1834	Delamination

Table 7 Correlation for fatigue of glass fiber specimens

Max stress (MPa)	Predicted cycles to failure		Measured cycles to failure	Failure mode
	fiber	1 mm Delam.		
862	6,934	8,475	13,873	fiber
984	2,141	1,104	3,033	fiber

in the number of cycles tested, whereas very little was observed. One explanation for this is that, for a given strain energy release rate, interfaces between 0- and ±45-deg plies are less susceptible to delamination than ones between 0-deg plies. A similar effect was reported previously for delamination of glass fiber specimens with cut central plies.[14] Under both static and fatigue tension loading it was found that specimens with discontinuous ±45-deg plies were relatively stronger than expected compared with specimens with discontinuous 0-deg plies.

Both types of carbon specimens delaminated, as expected. Damage starts very early and develops progressively. It is therefore necessary to consider delamination rates rather than cycles to failure. The delamination was similar to that observed in simpler specimens under static loading, starting at cracks in the resin pockets and propagating into the thick section. For both types of specimen delamination started at the forwardmost 0-deg plies, and no delamination occurred at any of the ±45-deg dropped plies. This confirms the greater susceptibility of the 0-deg plies to delamination under fatigue loading, as also found for static loading.

Failure Predictions

The predicted and measured static strengths are compared in Table 6. Fiber failure predictions are based simply on the net section stress. For the two cases that failed due to fiber fracture, the predictions are quite good and should be satisfactory for design purposes. However, to be conservative it would be necessary to apply a strength reduction factor.

For the case failing due to delamination the results are also good, with the prediction being conservative by about 5%. It was previously noticed that thicker specimens tended to show higher effective fracture energies than thinner ones.[12] A greater degree of conservatism might therefore have been expected in using data from a 10-ply specimen to predict failure of much thicker specimens. The reasons for the thickness effect are not understood. One possible explanation is that it is due to differing amounts of resin loss during the cure. Although the specimens tested in the present paper are relatively thick, delamination occurred quite close to the surface, and so it could be argued that they would be expected to behave more like thinner specimens. Further investigation of this effect is needed.

Under fatigue loading delamination occurs progressively with no significant initiation phase. Therefore, to predict fatigue life, it is necessary to choose a maximum acceptable amount of delamination beyond which the specimen is considered to have failed. In many applications no significant delamination is tolerated. A figure of 1 mm is convenient and is of the order of the smallest delamination that is likely to be detectable, and so this is used here.

Table 7 shows the predicted cycles to failure for the glass fiber specimens based on the 1 mm delamination criterion. Fiber fatigue predictions are also shown, based simply on the net section stress and plain specimen fatigue data. Comparison with the experimental values shows that the predictions are good and conservative in both cases.

Table 8 Correlation for fatigue of carbon fiber specimens

Specimen type	Max stress (MPa)	No. of cycles	Predicted delam. (mm)	Longest crack (mm)
1	1063	10,000	1.0	2.4
1	757	1,000,000	1.0	1.3
1	638	10,000,000	1.0	0.5
2	928	10,000	1.0	1.7
2	660	2,319,501	2.3	1.1

For the carbon specimens, which all delaminated, comparisons based on predicted vs measured delamination crack lengths are given in Table 8. The predictions are based on the delamination rates given in Table 2. The comparison is very good. For the cases at 10^4 cycles some of the cracks were slightly longer than predicted. However, for each delamination there are four edge cracks, and the values given in Table 8 are for the longest. If the four values are averaged, the maximum value of average delamination length is only 1.6 mm compared with a predicted length of 1 mm. It should also be noted that on each specimen there are four locations where delamination is expected, one on each side at each end. Crack lengths reported are for the location where most delamination occurred. At higher numbers of cycles the comparison is very close. Based on the maximum value of average delamination length rather than the longest crack, all of the predictions are conservative.

Overall these results show that satisfactory predictions can be made for both static and fatigue strength of tapered composites loaded in tension. Net section stresses enable a reasonable estimate of fiber failure to be made. The simple equation for strain energy release rate and values of fracture energy deduced from unidirectional specimens with cut central plies enable static delamination to be predicted. Similar specimens tested in fatigue allow delamination rates to be established and used to predict cyclic stresses that can be sustained without significant delamination occurring. This approach looks promising as the basis for designing tapered sections. Further work is required to investigate its application to other cases including compression loading and situations where out-of-plane as well as in-plane loading is present.

VII. Conclusions

Rapidly tapered sections of glass fiber epoxy failed due to fiber breakage under both static and fatigue loading. No delamination occurred. Failures initiated near the first dropped ply from the thin section. Close to net section strength was achieved under both static and fatigue loading.

Carbon fiber tapered specimens loaded statically failed by fiber fracture for the first type and delamination for the second type. Under fatigue loading both specimen types failed by delamination. In all cases delamination occurred at the dropped 0-deg plies nearest the thin section. It started with a crack in the resin pocket in front of the terminating plies and propagated above and below the dropped plies into the thick section. No delamination occurred into the thin section. In fatigue, delamination started immediately, with no significant initiation phase, and so it is necessary to consider delamination rates rather than fatigue lives. Close to net section static strength was achieved, but there was a significant reduction in fatigue strength due to delamination.

The most significant factor affecting strength is the number of plies dropped together. Specimens with plies dropped singly were found to be stronger than those with multiple plies dropped together despite having a steeper taper angle. Unidirectional dropped plies are much more susceptible to delamination than ±45-deg plies. To achieve maximum strength 0-deg plies should be dropped singly, and ±45-deg plies in single pairs, with continuous plies interleaved between the terminating plies.

Satisfactory strength predictions can be made for both static and fatigue tension loading. Fiber direction strength can be predicted based simply on the net section strength. Delamination strength can be calculated based on an equation for strain energy release rate and experimental data from unidirectional specimens with cut central plies. This approach looks promising as the basis for a general method for designing tapered composites.

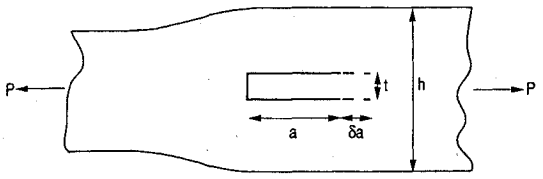

Fig. A1 Assumed delamination for strain energy release rate calculation.

Appendix: Equation for Strain Energy Release Rate

Consider the tapered section shown in Fig. A1. It is subject to a load per unit width P. A delamination length a is assumed to be present on both sides of the block of plies of thickness t. Once the delamination reaches a certain length, the effect of a further propagation δa is to unload a volume $t.\delta a$ and to increase the stress in a volume $(h-t).\delta a$. The local stress field does not affect the strain energy release rate because it moves along the specimen. This also assumes that no load is transferred into the delaminated plies due to friction between the continuous and discontinuous plies at the start of the taper.

The change in strain energy per unit width for the propagation δa is given by

$$\delta U = \delta a P^2/2K^* - \delta a P^2/2K_0 \tag{A1}$$

where K_0 is the original in-plane stiffness per unit width defined as the axial force per unit width for unit applied axial strain, and K^* is the stiffness after delamination assuming the delaminated plies carry no load.

For delamination under constant displacement there is no external work, and so the strain energy release rate G is equal to the change in strain energy per unit area of delamination

$$G = \delta U/2\delta a \tag{A2}$$

Substituting into Eq. (A1) gives

$$G = P^2/4(1/K^* - 1/K_0) \tag{A3}$$

Rearranging

$$G = P^2(K_0 - K^*)/4K_0K^* \tag{A4}$$

Finite element analysis has confirmed that this constant value of strain energy release rate is reached very quickly, after a propagation distance of the order of only about t.[12]

Acknowledgments

The authors would like to acknowledge the support of the United Kingdom Science and Engineering Research Council and Westland Helicopters for this research under Contract no. GR/F/28687.

References

[1]Kemp, B. L., and Johnson, E. R., "Response and Failure Analysis of a Graphite-Epoxy Laminate Containing Terminating Internal Plies," *Proceedings of the AIAA/ASME/ASCE/AHS 26th Structures, Structural Dynamics and Materials Conference* (Orlando, FL), AIAA, New York, 1985, pp. 13–24 (AIAA Paper 85-0608).

[2]Curry, J. M., Johnson, E. R., and Starnes, J. H., "Effect of Dropped Plies on the Strength of Graphite-Epoxy Laminates," *Proceedings of the AIAA/ASME/ASCE/AHS 28th Structures, Structural Dynamics, and Materials Conference* (Monterey, CA), AIAA, Washington, 1987, pp. 737–747 (AIAA Paper 87-0874).

[3]Lagace, P. A., and Cannon, R. K., "Effects of Ply Dropoffs on the Tensile Behavior of Graphite/Epoxy Laminates," *4th Japan/US Conference on Composite Materials*, Washington, June 1988, pp. 1–11.

[4]Hoa, S. V., Daoust, J., Du, B. L., and Vu-Khanh, T., "Interlaminar Stresses in Tapered Laminates," *Polymer Composites*, Vol. 9, No. 5, 1988, pp. 337–343.

[5]Salpekar, S. A., Raju, I. S., and O'Brien, T. K., "Strain Energy Release Rate Analysis of Delamination in a Tapered Laminate Subjected to Tension Load," *Proceedings of the American Society for Composites 3rd Technical Conference*, Seattle, 1988, pp. 642–654.

[6]Fish, J. C., and Lee, S. W., "Delamination of Tapered Composite Structures," *Engineering Fracture Mechanics*, Vol. 34, No. 1, 1989, pp. 43–54.

[7]Botting, A. D., Vizzini, A. J., and Lee, S. W., "The Effect of Ply-Drop Configuration on the Delamination Strength of Tapered Composite Structures," *Proceedings of the AIAA/ASME/ASCE/AHS 33rd Structures, Structural Dynamics, and Materials Conference* (Dallas, TX), AIAA, Washington, DC, 1992.

[8]Davila, C. G., and Johnson, E. R., "Analysis for Delamination Initiation in Postbuckled Dropped-Ply Laminates," *Proceedings of the AIAA/ASME/ASCE/AHS 33rd Structures, Structural Dynamics, and Materials Conference* (Dallas, TX), AIAA, Washington, DC, 1992, pp. 29–39.

[9]Webb, J. N., "Tensile Fatigue of a CFRP Specimen Containing a Change in Thickness," Royal Aircraft Establishment, RAE TR82072, Farnborough, England, UK, 1982.

[10]Fish, J. C., and Vizzini, A. J., "Delamination of Ply-Dropped Configurations," American Society for Testing and Materials 11th Symp. on Composite Materials: Testing and Design, May 1992.

[11]Murri, G. B., Salpekar, S. A., and O'Brien, T. K., "Fatigue Delamination Onset Prediction in Tapered Composite Laminates," NASA TM101673, 1989.

[12]Wisnom, M. R., "Delamination in Tapered Unidirectional Glass Fiber-Epoxy Under Static Tension Loading," *Proceedings of the AIAA/ASME/ASCE/AHS 32nd Structures, Structural Dynamics, and Materials Conference* (Baltimore, MD), AIAA, Washington, DC, 1991, pp. 1162–1172 (AIAA Paper 91-1142).

[13]Wisnom, M. R., "Prediction of Delamination in Tapered Unidirectional Glass Fiber-Epoxy with Dropped Plies under Static Tension and Compression," Specialists Meeting on Debonding/Delamination of Composites, AGARD CP530, Patras, Greece, May 1992.

[14]Wisnom, M. R., Jones, M. I., and Cui, W., "Delamination in Composites with Terminating Internal Plies Under Tension Fatigue Loading," American Society for Testing and Materials Fifth Symposium on Composite Materials: Fatigue and Fracture, ASTM STP 1230, Atlanta, GA, May 1993.